Nanomagnetic actuation of receptor-mediated signal transduction

ROBERT J. MANNIX[1†], SANJAY KUMAR[1,2†], FLÁVIA CASSIOLA[1], MARTÍN MONTOYA-ZAVALA[1], EFRAIM FEINSTEIN[3], MARA PRENTISS[3] AND DONALD E. INGBER[1*]

[1]Vascular Biology Program, Departments of Pathology and Surgery, Harvard Medical School and Children's Hospital, Boston, Massachusetts 02115, USA
[2]Department of Bioengineering, University of California, Berkeley, California 94720, USA
[3]Department of Physics, Harvard University, Cambridge, Massachusetts 02138, USA
[†]These authors contributed equally to this work.
[*]e-mail: donald.ingber@childrens.harvard.edu

Complex cell behaviours are triggered by chemical ligands that bind to membrane receptors and alter intracellular signal transduction. However, future biosensors, medical devices and other microtechnologies that incorporate living cells as system components will require actuation mechanisms that are much more rapid, robust, non-invasive and easily integrated with solid-state interfaces. Here we describe a magnetic nanotechnology that activates a biochemical signalling mechanism normally switched on by binding of multivalent chemical ligands. Superparamagnetic 30-nm beads, coated with monovalent ligands and bound to transmembrane receptors, magnetize when exposed to magnetic fields, and aggregate owing to bead–bead attraction in the plane of the membrane. Associated clustering of the bound receptors acts as a nanomagnetic cellular switch that directly transduces magnetic inputs into physiological cellular outputs, with rapid system responsiveness and non-invasive dynamic control. This technique may represent a new actuator mechanism for cell-based microtechnologies and man–machine interfaces.

Microdevices containing microelectrode arrays have been developed to influence the activity of neurons and myocytes with electrical stimuli[1,2], but this approach cannot be used in the control of microsystems containing non-excitable cells. Therefore an alternative to electrical actuation would be highly desirable, particularly one that is more robust, chemically specific and lower in power. We therefore set out to develop a strategy to rapidly and reversibly control a much wider range of transmembrane signal transduction pathways using a nanoscale magnetic actuation mechanism that would be broadly applicable to a vast array of cell types and receptor systems. The concept is simple—magnetic forces are used in combination with receptor-bound magnetic nanobeads to physically promote receptor clustering and thereby mimic oligomerization-dependent activation mechanisms, which are induced by binding of natural multivalent chemical ligands to cell surface receptors.

Mast cells perform immune surveillance in living tissues by expressing plasma membrane FcεRI receptors that engage Fc portions of single IgE molecules. When they are not activated, mast cells present these receptor–antibody complexes individually (unclustered) on their surface membrane for extended periods of time[3]. When multivalent antigens (immunogens) bind to the exposed variable portion of these bound IgE molecules, they induce FcεRI receptor oligomerization. Receptor clustering triggers an intracellular signalling response characterized by a rapid rise in cytosolic calcium due to influx from the extracellular space and release from intracellular stores[4]; this chemical messenger, in turn, triggers vesicle degranulation and histamine release, which initiate the local inflammatory response[5].

To determine whether we could harness this mechanism using a magnetic nanotechnology, we pre-incubated RBL-2H3 mast cells with IgE directed against the dinitrophenyl (DNP) antigen so that these 'primed' cells would present these antibodies on their surface bound to FcεRI receptors. Treatment of cells with a bolus of soluble horse serum albumin derivatized with multiple DNP moieties (DNP-HSA) resulted in a transient threefold increase in mean cytosolic calcium within 1–2 min of addition (Fig. 1a), consistent with previous reports in these cells[6]. In contrast, addition of soluble monovalent DNP-lysine (DNP-Lys) failed to activate a calcium signalling response (Fig. 1a). Moreover, when DNP-HSA was added to cells pre-treated with excess DNP-Lys, calcium signalling was completely inhibited (see Supplementary Information, Fig. S1), confirming that soluble monovalent ligands bind to these receptors. Thus, multivalency, and not ligation alone, is required for FcεRI receptor activation.
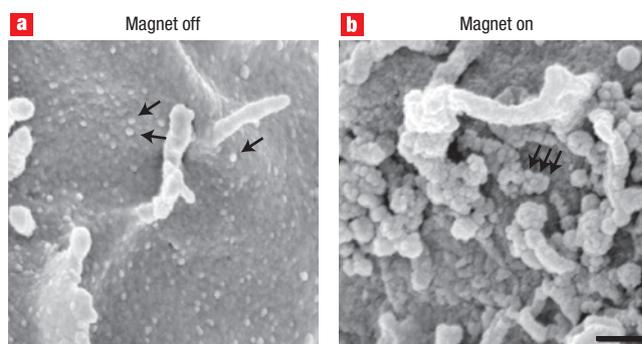
Superparamagnetic nanoparticles (30 nm in diameter) covalently conjugated to approximately 30 DNP-Lys ligands per bead were then added to cells pre-treated with anti-DNP IgE. Binding of these multivalent nanobeads to cell surface IgE–FcεRI receptor complexes resulted in activation of a similar threefold increase in intracellular calcium, but with even faster dynamics (compare Fig. 1b and 1a). Importantly, when the antigen density of each nanobead was reduced to approximately three DNP ligands per bead, calcium signalling was significantly suppressed, and when it was reduced to one DNP per bead, there was no detectable response (Fig. 1b). Beads coated with one DNP per bead did, however, bind to cell surface receptors, as confirmed by scanning electron microscopy (SEM), which demonstrated isolated 30-nm beads distributed evenly across the plasma membrane in the absence of an applied magnetic field (Fig. 2). Quantitative examination of 20 SEM images of different cells confirmed that more than 95% of control cells displayed only
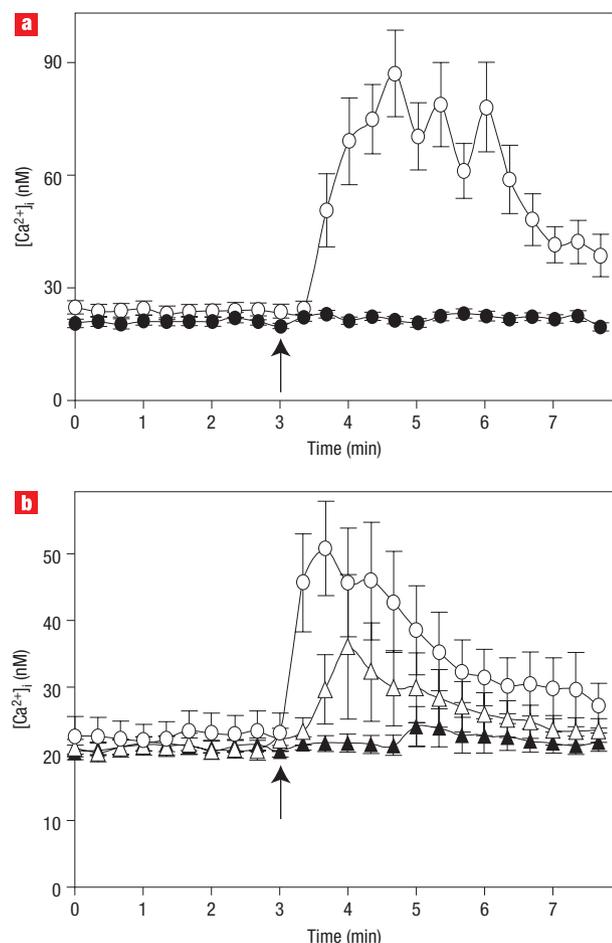
Figure 1 Activation of intracellular calcium signalling by crosslinking surface-bound IgE antibodies. **a**, Changes in intracellular calcium concentration $[Ca^{2+}]_i$ in RBL-2H3 mast cells in which surface membrane $Fc\varepsilon RI$ receptors were preloaded with anti-DNP IgE antibodies. Changes in calcium concentration were measured using Fura-2 ratiometric imaging and induced by adding soluble multivalent DNP-HSA (100 ng ml^{-1}, open circles) or soluble monovalent DNP-Lys (100 μg ml^{-1}, filled circles). **b**, Signalling induced by adding magnetic nanobeads (30 nm diameter) coated with 30 (open circles), 3 (open triangles) or 1 (filled triangles) DNP per bead. Arrows indicate the time at which the soluble DNP (**a**) and DNP-coated magnetic nanobeads (**b**) were added.

Figure 2 Visualization of magnetically-induced clustering of single DNP-coated nanobeads with an electron microscope. **a**,**b**, Mast cells were pre-treated with anti-DNP IgE overnight to load the $Fc\varepsilon RI$ receptors, incubated with monovalent DNP beads (30 nm) for 3 h, washed free of unattached beads, fixed before (**a**) or after (**b**) application of electromagnetic force (1 A) for 2 min, and imaged with scanning electron microscopy. Arrows in **a** indicate individual bound nanobeads distributed over the cell surface in the absence of the electromagnetic force, which cluster as large aggregates as shown in **b** when the magnetic switch is activated (scale bar, 300 nm).

well-scattered, single attached beads. Thus, binding of magnetic nanobeads coated with monovalent DNP ligands to $Fc\varepsilon RI$ receptors does not activate intracellular calcium signalling, presumably because they fail to cluster and crosslink neighbouring receptors.

Based on these findings, we reasoned that we could create a magnetic cellular switch to control calcium signalling in these cells by applying magnetic fields to magnetize the bound superparamagnetic nanobeads and thus physically induce cohesion and aggregation of nanobead–receptor complexes on the cell membrane (Fig. 3a). To accomplish this, cells were pretreated with IgE overnight, incubated with superparamagnetic nanobeads (1 DNP/bead) for 3 h, washed free of unbound beads, and then exposed to magnetic fields applied using an electromagnetic needle[7,8]. The tip of the needle was placed near (<300 μm) the surface of cultured cells, and electrical pulses of increasing current (0.1, 0.3 and 1 A) were applied to the electromagnet for
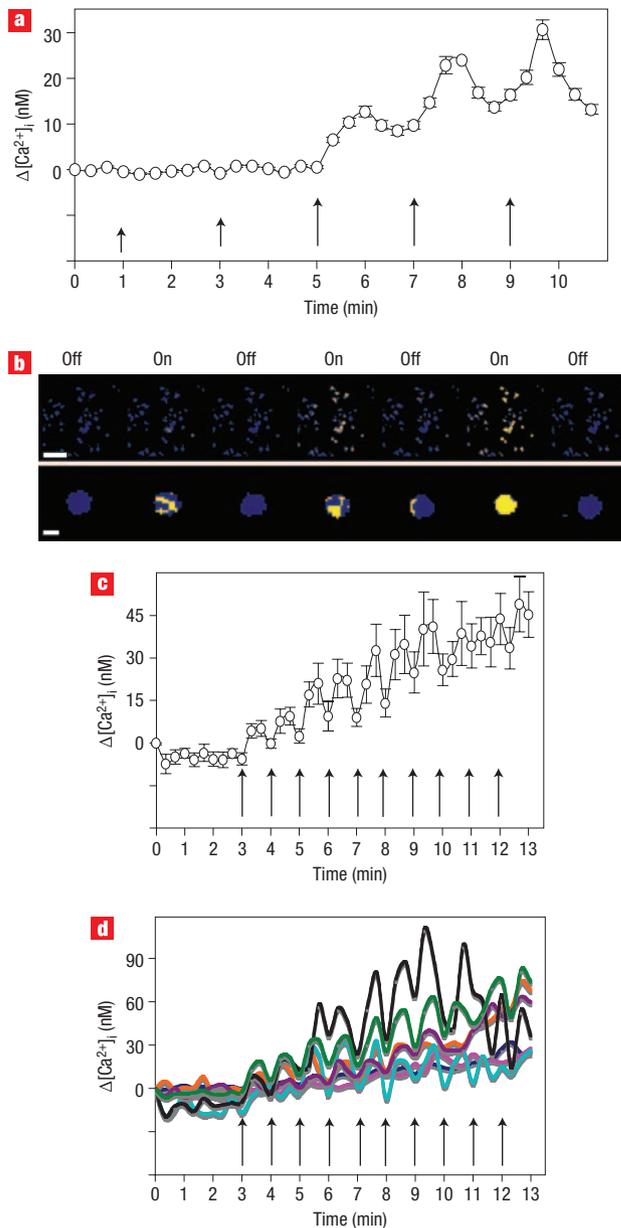
1 min separated by 1 min rest periods. Microfluorimetry revealed that a rapid rise in intracellular calcium was produced by the highest field strength (Fig. 3b and Fig. 4a). Calcium levels rose more than 120 nM in some cells located within $\sim$10 μm of the tip of the needle, and there was a sharp dependence of this calcium signalling response on the proximity of the cell to the needle tip (Fig. 3c). This spatial response closely mirrors the magnetic field strength, which also drops steeply as a function of distance from the magnet[9].

Importantly, SEM analysis confirmed that the receptor-bound nanobeads that appeared evenly distributed across the surface membrane of control cells aggregated into large closely packed clusters on the cell surface when the highest magnetic field was applied (Fig. 2b). Quantitative analysis of nearest-neighbour distances between 300 bead–bead pairs in five SEM images of different cells revealed that the separation distance was less than one bead diameter (27.7 ± 1.7 nm) before application of the magnetic field. Importantly, finite-element modelling of the forces exerted on individual beads and between neighbouring beads under these conditions confirmed that at the microneedle–bead separation distance used in this study (>30 μm), the magnitude of the tangential attractive force between neighbouring beads was more than an order of magnitude larger than the normal (tensional) force exerted on each nanobead (see Supplementary Information, Fig. S2). Moreover, the magnitude of the normal force on the beads was less than 10^{-17} N, which is many orders of magnitude smaller than the pN- to nN-scale forces that are required to induce conventional 'mechanosensitive' signalling through integrins[8,22] or stress-sensitive ion channels[23]. In contrast, application of similar magnetic fields to cells treated with DNP-coated nanobeads that lacked bound IgE, or to IgE-presenting cells pre-treated with uncoated nanobeads, consistently failed to induce a calcium response (see Supplementary Information, Fig. S3). Thus, activation of calcium signal transduction is not due to needle placement, heat generation or other nonspecific effects that can occur with use of extremely low-frequency magnetic fields[10]; rather, it depends directly on the intensity and distribution of the applied magnetic field.
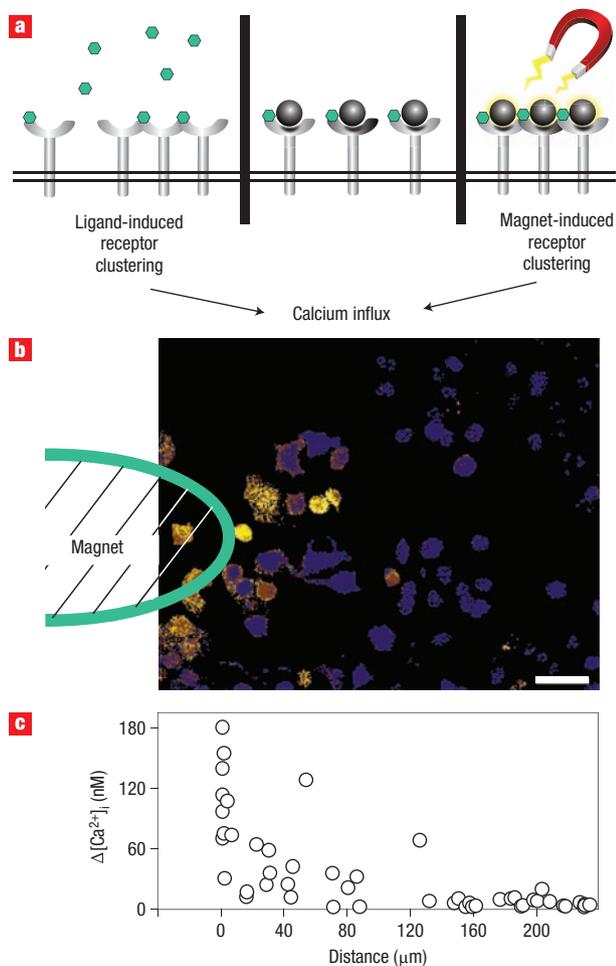
Figure 3 Nanomagnetic control of receptor signal transduction. a, The biochemical mechanism that stimulates downstream signalling (left) involves the binding of multi-valent ligands (small green hexagons) that induce oligomerization of individual IgE/FcεRI receptor complexes. In the magnetic switch, monovalent ligand-coated magnetic nanobeads (dark grey circles), similar in size to individual FcεRI receptors, bind individual IgE/FcεRI receptor complexes without inducing receptor clustering (centre). However, applying a magnetic field that magnetizes the beads and pulls them into tight clusters (right) rapidly switches on receptor oligomerization and calcium signalling. **b**, The pseudocoloured microfluorimetric image shows the local induction of calcium signalling (yellow) in cells near the tip of the electromagnet within 20 s of the field (1 A) being applied. Scale bar, 50 μm. **c**, Quantification of peak changes in intracellular calcium relative to time 0 ($\Delta[Ca^{2+}]_i$) measured within individual cells during a 1-min pulse of applied magnetic force (1 A) as a function of the distance of the tip from the cell surface.

Figure 4 Dynamic responsiveness and reversibility of magnetically induced receptor signalling. Mast cells were pretreated with anti-DNP IgE and monovalent DNP-coated nanobeads and subjected to time-dependent magnetic forces. **a**, Magnetic control over changes in intracellular calcium ($\Delta[Ca^{2+}]_i$) by applying five electromagnetic pulses of 1-min duration (0.1 A, 0.3 A, 1 A, 1 A and 1 A, arrows) separated by 1-min rest periods (mean $\pm$ standard error). **b**, Low (top; scale bar, 100 μm) and high (bottom; scale bar, 10 μm) magnification views of pseudocoloured microfluorimetric images showing repeated on- and off-switching of calcium signalling in groups of cells (top) and individual cells (bottom) that precisely coincide with activation and deactivation of the magnetic field, respectively. **c**, Effect of a more rapid cyclical magnetic stimulation regimen (40 s on, 20 s off; 1 A) on intracellular calcium signalling. **d**, $[Ca^{2+}]_i$ changes measured in individual cells from the study shown in panel **c**. Arrows in **c** and **d** indicate the start of magnetic pulses.

Microfluorimetry also revealed that calcium levels decrease within seconds of attenuating the magnetic pulse, and that calcium waves can be repeatedly induced in the same cells by re-administering magnetic pulses (at 1 A) (Fig. 4a,b; see also Supplementary Information, Movie 1). Even tighter coupling between stimulus and response was obtained by sequentially stimulating the cells with 40-s magnetic pulses separated by 20-s rest periods. This resulted in an oscillating pattern of multiple calcium waves with a frequency response that closely matched that of the electromagnetic stimulus, both within whole populations (Fig. 4c) and in individual cells (Fig. 4b,d), although gradual accumulation of intracellular calcium was observed in

most cells. Thus, magnetic fields can be used to selectively activate a rapid calcium signalling response and to produce controlled calcium oscillations by harnessing natural transmembrane receptor signalling mechanisms in living cells.

Magnetic fields have been used in the past in conjunction with micrometre-scale magnetic particles bound to cell surface integrin receptors to activate mechanosensitive signalling responses, including calcium influx through stress-sensitive ion channels[11,12]. However, these approaches are distinct from the switch described here, because use of microscale beads coated with multivalent integrin ligands promotes baseline receptor clustering and signal activation, in the absence of mechanical stimulation. In contrast, use of nanometre-sized magnetic beads coated with monovalent ligands that are on the same scale as individual receptors is critical to harness molecular signal transduction mechanisms that require receptor oligomerization for functional control in living cells. These smaller (30-nm) beads remain dispersed when bound to individual receptors under baseline conditions and, because of their superparamagnetic properties, they only become magnetized and physically agglomerate into clusters that activate signal transduction in the presence of an applied magnetic field. This nanomagnetic cellular switch is also novel in that it can be maintained in an inactive state for extended periods of time (hours to days), and then rapidly switched on and off dynamically in response to oscillating magnetic signals.

The requirement for receptor clustering for activation of signal transduction is a hallmark of many types of receptors, including ones that bind immunogens[13], cytokines[14], neurotransmitters[15] and metabolites[16]. Thus, this new magnetic nanotechnology, which can make use of any type of surface membrane receptor that requires a multivalent ligand for signal activation, opens many new avenues to control cellular metabolism using non-invasive magnetic control. For example, because this magnetic cellular switch permits the transduction of magnetic inputs into biological signals with precise spatiotemporal control, it represents a potentially valuable tool to control the behaviour of living cellular components within the microtechnologies and biochips that are beginning to be used in biomedical devices, sensors, drug delivery systems and other types of man–machine interfaces. It also offers the ability to add similar functionality to other multifunctional imaging nanotechnologies that are designed to control spatial assembly of cells[17] or to simultaneously localize diseased tissues (for example, tumours), release therapeutics and monitor response to therapy[18]. In fact, ligand-conjugated superparamagnetic nanoparticles have been approved for clinical use as contrast agents in magnetic resonance imaging[19]. Thus, it may be possible to use this type of cellular magnetic switch in conjunction with transdermal magnetic fields to control cellular functions *in vivo*, including immunological responses, in the future. All of these technologies are in their infancy, and their scope and impact could be extended dramatically with the use of magnetic control elements capable of actuating specific transmembrane receptor signalling mechanisms at precise times and locations. By providing a non-invasive method to convert magnetic inputs into receptor-specific biological outputs, this nanotechnology-based receptor actuation mechanism represents an important first step towards this form of magnetic cellular control.

METHODS

CELL CULTURE

Rat basophilic leukaemia RBL-2H3 mast cells (American Type Culture Collection, Manassas) were cultured in Dulbecco's modified Eagle's medium (DMEM) supplemented with 10 mM N-2-hydroxyethylpiperazine-N-2-ethanesulphonic acid (Hepes), 2 mM L-glutamine, 100 U ml^{-1} penicillin, 100 µg ml^{-1} streptomycin and 10% fetal bovine serum (Invitrogen) at 37 °C under 5% CO_2. For calcium ratiometric imaging, cells were seeded sparsely on coverglass-bottomed 35-mm dishes (MatTek) and cultured for 24 h. Mouse monoclonal anti-DNP IgE antibodies (Clone SPE-7, Sigma-Aldrich) were added

(63 µg ml^{-1}) and cells were cultured overnight. Cells were then washed twice with DMEM supplemented with 1% bovine serum albumin (Intergen; Cohn fraction V) and 20 mM Hepes buffer, pH 7.4 (DMEM-BSA) to remove unbound IgE antibodies and serum components. The magnetic nanobeads were then added to the cells (1.25×10^{13} nanobeads ml^{-1}) with 10 µM Fura2-AM in DMEM-BSA for 3 h at 37 °C. Cells were washed free of non-adherent nanobeads and excess Fura2-AM before analysis by multiple washes in DMEM-BSA and Hank's Balanced Salt Solution supplemented with 1% BSA and 20 mM Hepes, pH 7.4. The washed cells were transferred into microscope analysis medium that maintains a stable pH under room air composed of Hank's salts-based Minimum Essential Medium (MEM; minus MEM vitamins and phenol red), 2 mM L-glutamine, 1 mM sodium pyruvate, 1% BSA, 10 µg ml^{-1} high-density lipoprotein (Bionetics Research), 5 µg ml^{-1} holo-transferrin (Collaborative Research) and 20 mM Hepes, pH 7.4.

IMAGING

Cytosolic calcium levels were quantified using microfluorimetry in cells cultured on an automated stage (LUDL Electronics Products) of a Nikon Diaphot 300 inverted microscope (Nikon USA) fitted with a quartz ×20 objective (0.5 NA) and a Polychrome II high-speed 75 W xenon lamp monochromator (TILL Photonics LLC) that illuminates cells with alternating 340 nm and 380 nm light for Fura2-AM dye excitation. The stage was heated to 37 °C using a custom-built stage heater (MVI) fitted with an Omega CN9000A heat controller (Omega Engineering). Emission fluorescence at 510 ± 40 nm was captured by an Orca 100 CCD 12-bit digital camera (Hamamatsu, Japan) with 4×4 pixel binning. Fura2-AM ratio images (340/380 nm) were produced at 20-s intervals between image pairs using image background subtraction and noise reduction functions of IPLab Ratio software (Scanalytics, BD Biosciences). Ratio images were converted into calcium concentrations based upon a standard curve generated in RBL-2H3 cells treated with 10 µM ionomycin at 37 °C in the presence of various calcium concentrations in 150 mM KCl buffer[20]; the K_d of Fura-2 binding to calcium was determined to be 225 nM in these cells.

For scanning electron microscopy studies, 2.5% glutaraldehyde was added to cells pre-incubated with IgE and monovalent DNP beads either before or after exposure to an electromagnetic pulse (1 A) for 1 min, and the magnetic field was maintained for an additional minute. Cells were post-fixed with 1% osmium tetroxide, sputter-coated with gold (4 nm), and images recorded using a Leo 982 field emission scanning electron microscope (LEO Electron Microscopy).

MAGNETIC NANOBEADS

Superparamagnetic nanobeads (30 nm diameter, 5 nm iron core) coated with 30 amine groups per bead by the manufacturer (Nanocs) were placed in an ultrasonic bath for 10 s at room temperature to ensure a single bead suspension before being coated at different ratios (0:30, 1:29, 3:27 and 30:0) of Nε-2,4-dinitrophenyl-L-lysine (DNP-lysine):L-lysine (Sigma-Aldrich) to vary the average number of DNP ligands per bead. The nanobeads were washed four times with 0.1 M 2-[N-morpholino]ethanesulphonic acid pH 6.3 buffer (MES buffer) and treated with 5% glutaraldehyde (Electron Microscopy Sciences) for 3 h at 25 °C in the same buffer to activate the surface amines. Beads were then washed, collected using MACS MS reversible magnetic steel wool columns (Miltenyi Biotec) and incubated (12 h, 4 °C) with a total of 100 µg of DNP- and L-lysine in 500 µl MES buffer. The reaction was quenched by adding 100 µl of 1 M ethanolamine (pH 8) and incubating for 1 h at 25 °C (ref. 21). The nanobeads were then collected in 500 µl distilled water, and 34 µl of ×10 phosphate buffered saline (without calcium or magnesium) was added to produce a slightly hypotonic solution to prevent nanobead aggregation. The coated beads were sonicated in a bath for 10 s at room temperature before being added to cells. In our studies, bead aggregation was not observed when DNP beads were used at dilutions of 1:4 or higher in culture medium.

MAGNETIC CONTROL OF CALCIUM SIGNALLING

Magnetic DNP beads adherent to cell surface FcεRI receptors through bound anti-DNP IgE antibodies were magnetized using a water-cooled, temperature-controlled electromagnetic microneedle[8] containing a 20-µm-diameter pole tip[7]. The electromagnetic needle was precisely positioned within the culture dish using an automated Micromanipulator (Eppendorf AG) so that the needle tip was visible within the high-power optical field, approximately 30 µm above the cell surface, at an angle of 45°, and not touching any cells. The magnetic field was controlled by manually switching the electric current supplied to the electromagnetic needle during ratio image capture using a regulated DC power supply (Summit Co., Korea).

LETTERS

References

1. Fromherz, P., Offenhausser, A., Vetter, T. & Weis, J. A neuron–silicon junction: a Retzius cell of the leech on an insulated-gate field-effect transistor. *Science* **252,** 1290–1293 (1991).
2. Young, T. H. & Chen, C. R. Assessment of GaN chips for culturing cerebellar granule neurons. *Biomaterials* **27,** 3361–3367 (2006).
3. Sutton, B. J. & Gould, H. J. The human IgE network. *Nature* **366,** 421–428 (1993).
4. Lu-Kuo, J. M., Joyal, D. M., Austen, K. F. & Katz, H. R. gp49B1 inhibits IgE-initiated mast cell activation through both immunoreceptor tyrosine-based inhibitory motifs, recruitment of src homology 2 domain-containing phosphatase-1, and suppression of early and late calcium mobilization. *J. Biol. Chem.* **274,** 5791–5796 (1999).
5. Segal, D. M., Taurog, J. D. & Metzger, H. Dimeric immunoglobulin E serves as a unit signal for mast cell degranulation. *Proc. Natl Acad. Sci. USA* **74,** 2993–2997 (1977).
6. Oka, T. *et al*. IgE alone-induced actin assembly modifies calcium signaling and degranulation in RBL-2H3 mast cells. *Am. J. Physiol. Cell Physiol.* **286,** C256–C263 (2004).
7. Matthews, B. D., LaVan, D. A., Overby, D. R., Karavitis, J. & Ingber, D. E. Electromagnetic needles with submicron pole tip radii for nanomanipulation of biomolecules and living cells. *Appl. Phys. Lett.* **85,** 2968–2970 (2004).
8. Matthews, B. D., Overby, D. R., Mannix, R. & Ingber, D. E. Cellular adaptation to mechanical stress: role of integrins, Rho, cytoskeletal tension and mechanosensitive ion channels. *J. Cell Sci.* **119,** 508–518 (2006).
9. Matthews, B. D. *et al*. Mechanical properties of individual focal adhesions probed with a magnetic microneedle. *Biochem. Biophys. Res. Commun.* **313,** 758–764 (2004).
10. McCreary, C. R., Dixon, S. J., Fraher, L. J., Carson, J. J. & Prato, F. S. Real-time measurement of cytosolic free calcium concentration in Jurkat cells during ELF magnetic field exposure and evaluation of the role of cell cycle. *Bioelectromagnetics* **27,** 354–364 (2006).
11. Glogauer, M., Ferrier, J. & McCulloch, C. A. Magnetic fields applied to collagen-coated ferric oxide beads induce stretch-activated Ca^{2+} flux in fibroblasts. *Am. J. Physiol.* **269,** C1093–C1104 (1995).
12. Meyer, C. J. *et al*. Mechanical control of cyclic AMP signalling and gene transcription through integrins. *Nature Cell Biol.* **2,** 666–668 (2000).
13. Bromley, S. K. *et al*. The immunological synapse. *Annu. Rev. Immunol.* **19,** 375–396 (2001).
14. Schreiber, A. B., Libermann, T. A., Lax, I., Yarden, Y. & Schlessinger, J. Biological role of epidermal growth factor-receptor clustering. Investigation with monoclonal anti-receptor antibodies. *J. Biol. Chem.* **258,** 846–853 (1983).
15. Kim, E., Cho, K. O., Rothschild, A. & Sheng, M. Heteromultimerization and NMDA receptor-clustering activity of Chapsyn-110, a member of the PSD-95 family of proteins. *Neuron* **17,** 103–113 (1996).
16. Rothberg, K. G., Ying, Y. S., Kamen, B. A. & Anderson, R. G. Cholesterol controls the clustering of the glycophospholipid-anchored membrane receptor for 5-methyltetrahydrofolate. *J. Cell Biol.* **111,** 2931–2938 (1990).
17. Tanase, M. *et al*. Assembly of multicellular constructs and microarrays of cells using magnetic nanowires. *Lab. Chip* **5,** 598–605 (2005).
18. Koo, Y. E. *et al*. Brain cancer diagnosis and therapy with nanoplatforms. *Adv. Drug Deliv. Rev.* **58,** 1556–1577 (2006).
19. Bulte, J. W. & Kraitchman, D. L. Iron oxide MR contrast agents for molecular and cellular imaging. *NMR Biomed.* **17,** 484–499 (2004).
20. Grynkiewicz, G., Poenie, M. & Tsien, R. Y. A new generation of Ca^{2+} indicators with greatly improved fluorescence properties. *J. Biol. Chem.* **260,** 3440–3450 (1985).
21. Song, J., Chen, J., Klapperich, C. M., Eng, V. & Bertozzi, C. R. Functional glass slides for *in vitro* evaluation of interactions between osteosarcoma TE85 cells and mineral-binding ligands. *J. Mater. Chem.* **14,** 2643–2648 (2004).
22. Overby, D. R., Matthews, B. D., Alsberg, E. & Ingber, D. E. Novel dynamic rheological behavior of individual focal adhesions measured within single cells using electromagnetic pulling cytometry. *Acta Biomaterialia* **1,** 295–303 (2005).
23. Sukharev, S. I., Sigurdson, W. J., Kung, C. & Sachs, F. Energetic and spatial parameters for gating of the bacterial large conductance mechanosensitive channel, MscL. *J. Gen. Physiol.* **113,** 525–540 (1999).

Author contributions

R.J.M. carried out experimental work, data analysis, method development, calcium analysis and wrote the paper. S.K. was responsible for experimental design, establishing the cell system and manuscript preparation. F.C. was involved with scanning electron microscopy and data analysis, M.M-Z. with electromagnetic needle construction and experimental work, and E.F. with finite-element modelling. M.P. supervised the design of the finite-element model, and D.E.I. devised the technology concept, supervised the project, and was involved in data interpretation and manuscript preparation.